Wall Effects in Convective Heat Transfer from a Sphere to Power Law Fluids in Tubes

Daoyun Song[*1], Rakesh K. Gupta[1] and Rajendra P. Chhabra[2]
[1]West Virginia University, [2]Indian Institute of Technology, Kanpur, India
*Corresponding author: Department of Chemical Engineering, West Virginia University, PO Box 6102, Morgantown, WV 26506, Daoyun.Song@mail.wvu.edu

Abstract: Heat transfer from a sphere having a uniform temperature and falling axially in a cylindrical tube filled with an incompressible power-law liquid is numerically investigated. The effects of varying the Reynolds number (Re), Prandtl number (Pr), power-law index (n), and the sphere-to-tube diameter ratio (λ) on the local and mean Nusselt numbers (Nu) have been extensively examined over the following ranges of conditions: $5 \le Re \le 100$, $1 \le Pr \le 100$, $0.2 \le n \le 1$, and $0 \le \lambda \le 0.5$. It was found that the wall effects on the mean Nusselt number diminish progressively with decreases in the power law index and the Reynolds number.

Keywords: Wall effects, Nusselt number, Power-law fluid, Sphere

1. Introduction

Heat transfer from a sphere to surrounding power law fluids is found to take place in various industrial processes, such as in thermal processing of foodstuffs, fixed and fluidized bed reactors, and slurry reactors. Although in most practical applications non-spherical particles and/or ensembles of particles are encountered, a thorough understanding of the hydrodynamic behavior of a spherical particle is germane to developing useful insights into the behavior of non-spherical particles and/or their clusters. Over the years, a considerable amount of literature has addressed the problem of fluid flow and heat transfer past a sphere in an unconfined region, especially in Newtonian fluids and to a limited extent in power-law fluids.[1-4] However, the flow over a sphere in a confined region is encountered in various applications such as falling ball viscometry, hydrodynamic chromatography, membrane transport, and hydraulic transport of coarse solids in pipes. A few authors[5-6] have taken into account the finite wall effect on flow and heat transfer, but this treatment is limited to Newtonian fluids. It should be noted that numerous fluids of industrial importance display shear-thinning characteristics which are conveniently approximated by the simple power-law model. Indeed, many of these fluids (polymer melts, polymer solutions, food emulsions, suspensions, and biological fluids) exhibit a value of the power-law index, n, typically in the range of ~0.2 and ~0.8.[7] Our recent work[8] has investigated the interplay between the degree of confinement and the power-law index on the drag from a sphere over wide ranges of the pertinent kinematic and physical parameters. This paper is a continuation of our previous work, and here the effects of confinement, power-law index, and changes in the Prandtl number on heat transfer are examined. In particular, the influences of sphere Reynolds number, Re varying from 5 to 100, the sphere-to-tube diameter ratio, λ varying from 0 to 0.5, the power-law index, n varying from 0.2 to 1, and the Prandtl number varying from 1 to 100 (maximum Pe=Pr.Re equals 4000) are elucidated on the Nusselt number.

2. Governing Equations

Consider a scenario in which a sphere with a diameter d located at the axis of a cylindrical tube having a diameter D falls at a steady velocity V_0 in a tube filled with a quiescent power-law liquid with a temperature T_0. This situation is tantamount to the fluid moving with a uniform velocity V_0 and temperature T_0 around the stationary sphere as shown schematically in Figure 1. Notice that the wall also moves at the same velocity V_0. Here, the boundary condition for temperature on the surface of the sphere is taken to be a constant temperature T_W, although it is slightly more complicated in practice. To simplify the model, the fluid is assumed to be incompressible with constant physical properties. In addition, viscous dissipation is neglected. It is worth mentioning that the assumption of consta-nt physical properties limits the application of these results to some moderate temperature difference between the sphere and the bulk fluid.

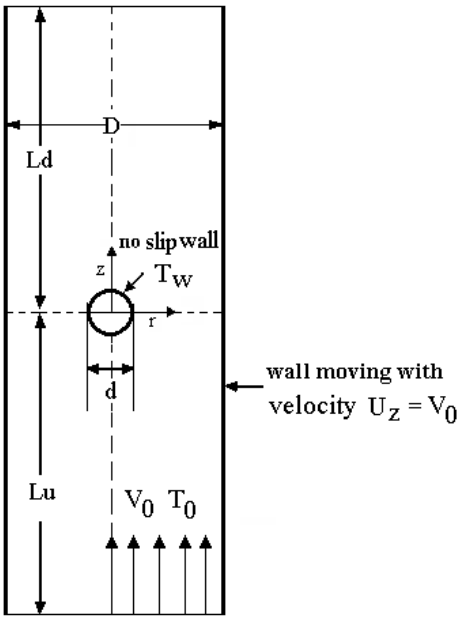

Figure 1. Schematic diagram of flow around a sphere in a tube.

For a two-dimensional, axisymmetric, steady flow in cylindrical coordinates, the governing equations in tensor form are as follows,

Continuity equation

$$\nabla \bullet U = 0 \tag{1}$$

Momentum equation

$$\rho U \bullet \nabla U = \nabla \bullet \sigma \tag{2}$$

Energy equation

$$\rho c_p U \bullet \nabla T = k \nabla^2 T \tag{3}$$

in which U, ρ, σ, c_p, T, and k are the velocity vector, fluid density, total stress tensor, specific heat, temperature and thermal conductivity, respectively. The total stress σ can be split into two parts, an isotropic pressure p and a deviatoric stress τ, i.e.,

$$\sigma = -pI + \tau \tag{4}$$

For incompressible power-law fluids, τ can be expressed as

$$\tau = \eta\left(\sqrt{I_2/2}\right)\dot{\gamma} = \left(m\left(\sqrt{I_2/2}\right)^{n-1}\right)\dot{\gamma} \tag{5}$$

where m is the consistency index, n is the power law index, and I_2 is the second invariant (a scalar) of the shear rate tensor, $\dot{\gamma} : \dot{\gamma}$. The shear rate tensor $\dot{\gamma}$ is defined by

$$\dot{\gamma} = \nabla U + (\nabla U)^T \tag{6}$$

Note that when n=1 and m=μ, Eq. (5) reduces to the Newtonian fluid constitutive equation. Substituting this equation into the momentum equation (2) yields the Navier-Stokes equation. The boundary conditions for the velocity and temperature variables are taken to be as follows,

(1) at the inlet

$U_r=0$, $U_z=V_0$, $T=T_0$

(2) on the tube wall

$U_r=0$, $U_z=V_0$, $\dfrac{\partial T}{\partial r} = 0$ (adiabatic)

(3) on the sphere surface

$U_r=U_z=0$, $T=T_W$

(4) At the axis of the tube

the position of r=0 is set to be one of axial symmetry

(5) At the exit

pressure is set to be zero and no viscous stress in implemented. The axial temperature gradient is set to zero, i.e., $\dfrac{\partial T}{\partial z} = 0$

Once the above governing equations along with the associated boundary conditions are numerically solved, the solutions are usually manipulated to compute some macroscopic quantities of interest. Here, it is useful to introduce some dimensionless numbers such as Re, Pr and Nu.

The Reynolds number for the falling sphere, Re is defined by

$$\mathrm{Re} = \frac{d^n V_0^{2-n} \rho}{m} \tag{7}$$

The Prandtl number, Pr is expressed as

$$\mathrm{Pr} = \frac{c_p m (V_0/d)^{n-1}}{k} \tag{8}$$

The local Nusselt number Nu_θ on the surface of the sphere is evaluated by

$$Nu_\theta = \frac{h_\theta d}{k} = \frac{d}{k(T_W - T_0)}\left(-k\frac{\partial T}{\partial N}\right)\Bigg|_\theta \quad (9)$$

in which h_θ is the local convective heat transfer coefficient, and N is the normal direction along the sphere surface. The local Nusselt number can be integrated over the entire sphere surface and the result divided by the sphere surface area to yield the mean Nu, which is given by

$$Nu = \frac{hd}{k} = \frac{1}{2}\int_0^\pi Nu_\theta \sin\theta d\theta \quad (10)$$

3. Numerical Solution Procedure

In this paper, the momentum equation and the energy equation, together with the above appropriate boundary conditions, were solved in a segregated manner using COMSOL Multiphysics software (version 3.5a). The flow geometry was drawn by means of the built-in CAD tools, and "quadrilateral" elements of the non-uniform grid were generated using the built-in meshing function of COMSOL Multiphysics as well. Lagrange-P_2P_1 scheme was chosen to handle the velocity-pressure coupling, while a Lagrange-Quadratic scheme was selected to approximate the elements when discretizing the energy equation. COMSOL modules utilizing the non-Newtonian power law viscosity model and heat convection and conduction were used. Details about solving the momentum equations are available in our previous paper.[8] The relative convergence tolerance of all the variables was set to 10^{-6}. Once the flow domain was mapped in terms of temperature, values of the global characteristic quantities such as the local or mean Nusselt numbers on the sphere surface were obtained through COMSOL postprocessing.

4. Results and Discussion

Before presenting the results, it is necessary to describe the choice of domain and grid employed. Based on previous experience, both the upstream Lu and the downstream Ld were taken to equal 65d. For computing results related to the unconfined situation, i.e., $\lambda=d/D=0$, a sphere-in-sphere configuration was utilized. The outer sphere radius, $R_\infty=500R$ was used to mimic the limiting case of $\lambda\to 0$. Except for this situation, a sphere-in-tube configuration was employed in all other cases. Computational details are available in our earlier work.[8]

4.1 Validation

In order to obtain confidence in the results, computations were first performed for heat transfer from an unconfined sphere to Newtonian liquids. These results are listed in Table 1 and are compared with the limited results available in the literature.[3,6,9,10] Kaviany[9] proposed the following equation to approximate the mean Nu,

$$\frac{Nu-1}{\left(\mathrm{Pr}+\frac{1}{\mathrm{Re}}\right)^{1/3}} = \mathrm{Re}^{0.41} \quad (11)$$

Another correlation was presented by Whitaker,[10]

$$Nu = 2 + \left(0.4\,\mathrm{Re}^{0.5} + 0.06\,\mathrm{Re}^{2/3}\right)\mathrm{Pr}^{0.4}\left(\frac{\mu_b}{\mu_0}\right)^{1/4} \quad (12)$$

Here, $(\mu_b/\mu_0)^{1/4}$ was taken to be unity based on the assumption of physical properties being independent of temperature. As can be seen from Table 1, our calculations of the mean Nusselt number are in good agreement with literature results.[6,9,10] In the presence of finite wall confinement, a similar comparison of average Nusselt numbers is tabulated in Table 2. Again, the present computational results agree very well with those obtained by Maheshwari et al.[6] Table 3 shows the comparison of local Nusselt numbers calculated by us with the results of Dhole et al.[3] at the front stagnation point ($\theta=0°$) and the rear stagnation point ($\theta=180°$) at $\lambda=0$ and Pr=10. For Newtonian fluids, both results are very close. However, they deviate as n decreases. It is not surprising that the difference becomes larger as n decreases. As n becomes smaller, the reliability and stability of numerical simulations are found to deteriorate.

Table 1. Comparison of average Nusselt number for an unbounded sphere (λ=0) at Pr=7

Re	Present work	Mahe-shwari et al.[6]	Eq. (11)	Eq. (12)
1	3.1001	3.103	2.999	3.002
5	4.691	4.691	4.734	4.33
10	5.857	5.859	5.938	5.36
50	10.486	10.545	10.517	9.94
70	11.964	12.089	11.922	11.51
100	13.874	14.155	13.939	13.53

Table 2. Comparison of average Nusselt number at Pr=7

	λ=0.1		λ=0.5	
Re	Present work	Mahe-shwari et al.[6]	Present work	Mahe-shwari et al.[6]
1	3.172	3.172	3.7	3.697
5	4.737	4.736	6.173	6.173
10	5.895	5.894	7.583	7.584
20	7.498	7.497	9.385	9.387
30	8.695	8.695	10.679	10.681
50	10.544	10.548	12.658	12.66
70	12.067	12.072	14.315	14.312
100	14.082	14.092	16.532	16.527

4.2 Effects of Reynolds number (Re), Diameter ratio (λ) and Prandtl number (Pr) on the local Nusselt number (Nu_θ)

Figure 2 shows the effects of Re, n and λ on the local Nusselt number on the sphere surface under the conditions of constant wall temperature and constant Pr of 20. For purposes of illustration, results are presented for Re equal to 10 and 100, n equal to 1, 0.6 and 0.3 and λ equal to 0, 0.2 and 0.5. The variation of local Nusselt number for Newtonian fluids exhibits markedly different behavior from that of shear-thinning fluids as shown in Figure 2. For Newtonian fluids, in the absence of vortex formation (Re=10), the local Nusselt number is relatively large at the front stagnation point (θ=0°), and it then decreases monotonically along the surface to a minimum at the rear stagnation point (θ=180°). When Re equals 100, and there is now flow separation and vortex formation, the Nusselt number decreases from its maximum value at the front stagnation point until near the separation point; beyond this, a progressive increase in Nusselt number is observed up to the rear stagnation point. By contrast, for shear-thinning fluids, whether for Re = 10 or Re = 100, as can be seen from Figure 2, the local Nusselt number first increases from θ=0° to approximately θ=30°, and then it decreases. Thereafter, the behavior is similar to that of Newtonian fluids, depending on the Reynolds number. In other words, the maximum Nusselt number for shear-thinning fluids is not at the front stagnation point, but somewhere away from it. In addition, this phenomenon is facilitated with the increasing degree of shear-thinning. A further examination of Figure 2 reveals the following information. The local Nusselt number, as expected, increases with Re. It also increases as n is gradually reduced below unity. As n decreases, the fluid becomes more shear-thinning, that is to say, the effective viscosity of liquid near the sphere decreases, increasing Re locally. This decrease in viscosity results in large velocity gradients near the sphere surface. As a consequence, convective heat transfer is promoted and the local Nusselt number increases. Apart from the above, a comparison of Figures 2(b) and 2(c) with Figure

Table 3. Comparison of local Nusselt number at λ=0 and Pr=10

Re	n	θ=0°		θ=180°	
		Present work	Dhole et al.[3]	Present work	Dhole et al.[3]
10	1	10.215	10.218	1.84	1.875
	0.8	10.538	10.457	1.803	1.854
	0.6	10.943	11.286	1.758	1.654
100	1	29.583	30.696	8.814	9.765
	0.8	30.742	31.979	8.763	9.061
	0.6	32.1	36.543	8.679	10.09

2(a) shows that the local Nusselt number increases with the severity of confinement. This can again be attributed to the changes in the velocity gradient near the sphere. With increasing degree of confinement, velocity gradients near the sphere become sharper,[8] which facilitates heat transfer. Therefore, the heat transfer problem is inherently connected with fluid flow. Finally, as expected, the local Nusselt number increases with the Prandtl number as shown in Figure 3.

It is necessary to point out that there exist kinks in the curves of the local Nusselt number when Pr becomes larger at n=0.2 as shown in Figure 4. These kinks may be due to a numerical instability. As mentioned before, the convergence and accuracy of numerical solutions are deteriorated as fluids become increasingly shear-thinning. This situation is aggravated at higher Prandtl numbers.

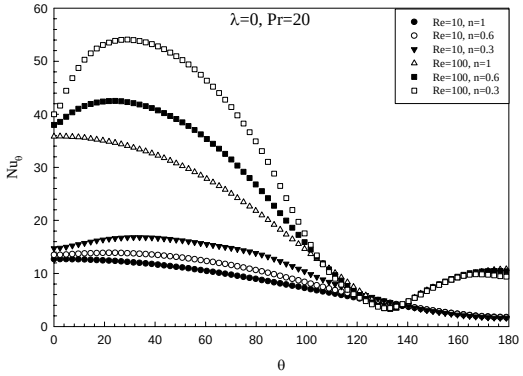

(a)

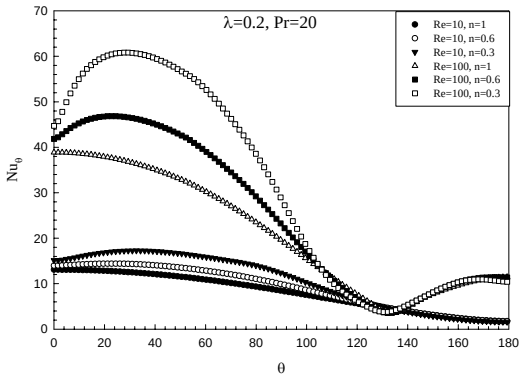

(b)

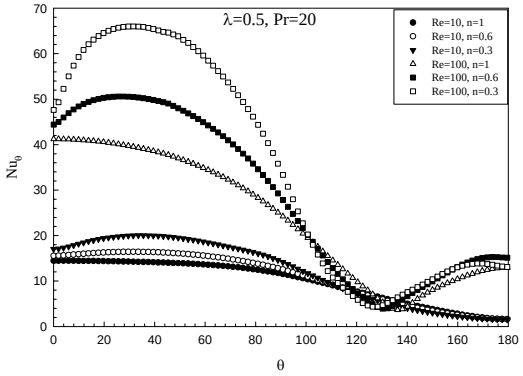

(c)

Figure 2. Local Nusselt number on the sphere surface at various Reynolds numbers and power law indices for (a) λ=0, (b) λ=0.2 and (c) λ=0.5

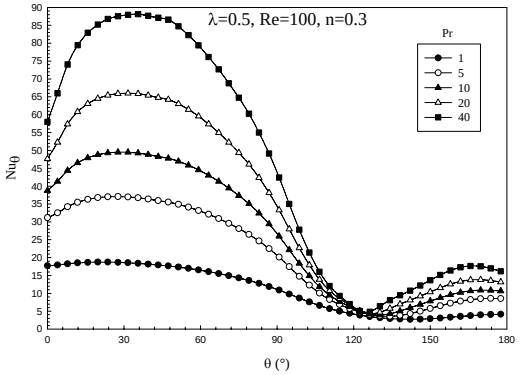

Figure 3. Local Nusselt number on the sphere surface at various Prandtl numbers

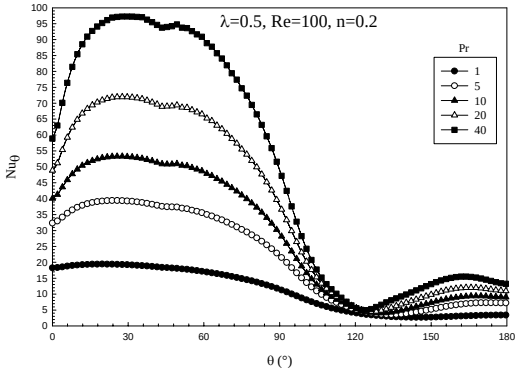

Figure 4. Local Nusselt number on the sphere surface at Re=100 and n=0.2

4.3 Effects of Reynolds number (Re), Diameter ratio (λ) and Prandtl number (Pr) on the mean Nusselt number (Nu)

Figures 5 and 6 show the effects of λ, Re and n on the mean Nusselt number at Pr=20 and 1, respectively. Both the local and average Nusselt numbers increase with increases in Re, Pr and λ and/or a decrease of n. An inspection on Figures 5 and 6 reveals that the wall effect is less severe in a more shear-thinning fluid at both low and high Prandtl numbers. This conclusion is similar to the effect on drag coefficient.[8] Additionally, the wall effect gradually diminishes with a decrease of Re. In particular, the wall effect is not appreciable at a low Pr and a small n as shown in Figure 6(c).

5. Conclusions

The governing equations for simultaneous flow around a confined sphere and heat transfer to power-law fluids were solved numerically using COMSOL Multiphysics. Extensive numerical results are reported here which delineate the effects of Reynolds number Re, power-law index n, tube-to-sphere diameter ratio λ, and the Prandtl number Pr on the local and average Nusselt numbers. The ranges of conditions: were: 5≤Re≤100, 0.2≤n≤1, 0≤λ≤0.5, and 1≤Pr≤100. In general, due to confinement, the fluid close to the sphere is subject to intense shearing. This lowers the effective viscosity and raises the Reynolds number locally. As a consequence the local Nusselt number increases as compared to the situation for the unconfined sphere. This has direct applications in thermal processing of food particles in carbopol solutions where the food particle to tube diameter ratio can be as high as 0.3 to 0.4. Therefore, an increase in the rate of heat transfer should translate into a shorter residence time or increased throughput for a specified experimental set-up.

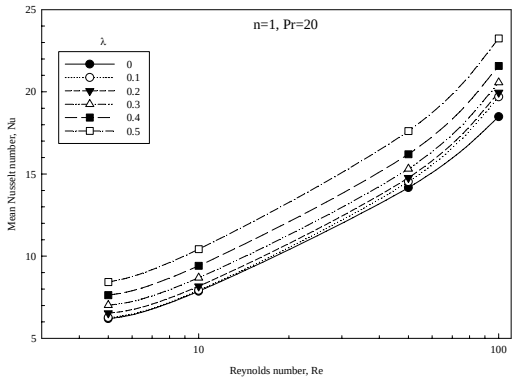

(a)

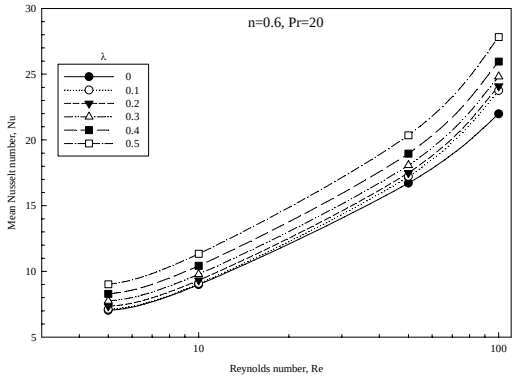

(b)

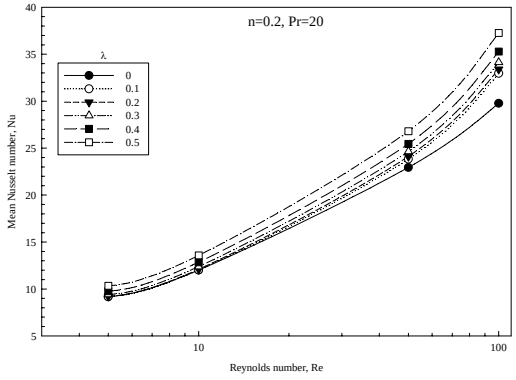

(c)

Figure 5. Dependence of mean Nusselt number on Re, λ and n at a constant Pr of 20 (a) n=1.0, (b) n=0.6 and (c) n=0.2

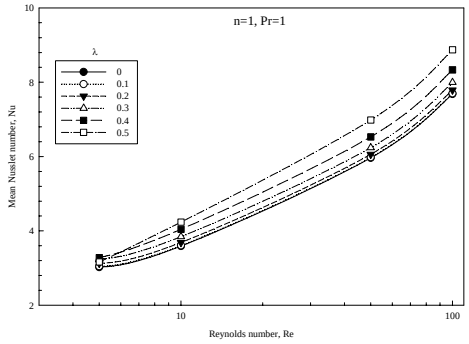

(a)

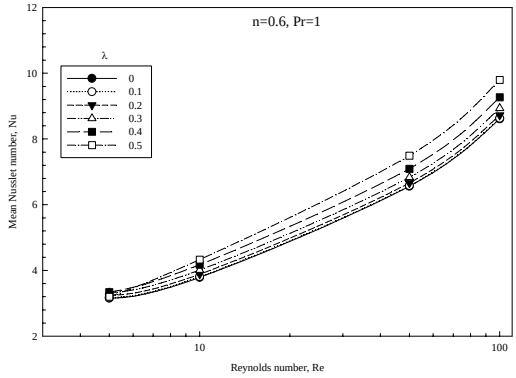

(b)

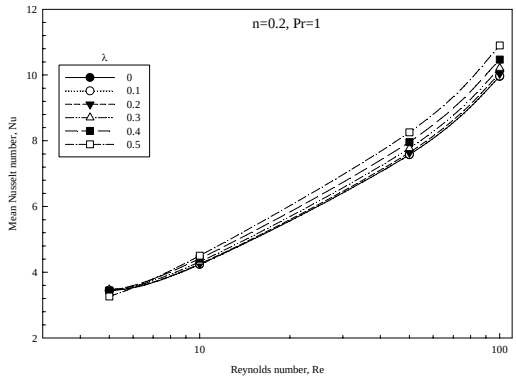

(c)

Figure 6. Dependence of mean Nusselt number on Re, λ and n at a constant Pr of 1 (a) n=1.0, (b) n=0.6 and (c) n=0.2

6. References

1. K. A. Missirlis, D. Assimacopoulos, E. Mitsoulis, R. P. Chhabra, Wall effects for motion of spheres in power-law fluids, *J. Non-Newtonian Fluid Mech.*, **96**, 459–471 (2001)

2. S. D. Dhole, R. P. Chhabra, V. Eswaran, Flow of power law fluids past a sphere at intermediate Reynolds numbers, *Ind. Eng. Chem. Res.*, **45**, 4773–4781 (2006)

3. S. D. Dhole, R. P. Chhabra, V. Eswaran, Forced convection heat transfer from a sphere to non-Newtonian power law fluids, *AIChE J.*, **52**, 3658-3667 (2006)

4. S. D. Dhole, R. P. Chhabra, V. Eswaran, A numerical study on the forced convection heat transfer from an isothermal and isoflux sphere in the steady symmetric flow regime, *Int. J. Heat Mass Transfer*, **49**, 984–994 (2006)

5. R. M. Wham, O. A. Basaran, C. H. Byers, Effects on flow past solid spheres at finite Reynolds numbers, *Ind. Eng. Chem. Res.* **35**, 864–874 (1996)

6. A. Maheshwari, R. P. Chhabra, G. Biswas, Effect of blockage on drag and heat transfer from a single sphere and an in-line array of three spheres, *Powder Technol.*, **168**, 74-83 (2006)

7. R. P. Chhabra, J. F. Richardson, *Non-Newtonian Flow and Applied Rheology*, 2nd ed., pp 249-314. Butterworth-Heinemann, Oxford (2008)

8. D. Song, R. K. Gupta, R. P. Chhabra, Wall effects on a sphere falling in quiescent power law fluids, *Ind. Eng. Chem. Res.*, **48**, 5845-5856 (2009)

9. M. Kaviany, *Principles of Convection Heat Transfer*, pp 354-358, Springer-Verlag, New York (1994)

10. S. Whitaker, Forced convection heat transfer correlations for flow in pipes, past flat plates, single cylinders, single spheres, and for flow in packed beds and tube bundles, *AIChE J.*, **18**, 361-371 (1972)